J Polym Res (2017) 24: 165
DOI 10.1007/s10965-017-1323-3

ORIGINAL PAPER

Synthesis, characterization and application of a novel nanometer-sized chelating resin for removal of Cu(II), Co(II) and Ni(II) ions from aqueous solutions

A. F. Shaaban[1] · **A. A. Khalil**[1] · **Mohamed Radwan**[2] · **Manal El Hefnawy**[2] · **H. A. El Khawaga**[2]

Received: 8 June 2017 / Accepted: 6 September 2017 / Published online: 17 September 2017

Abstract A novel nanometer-sized chelating resin (NSCR) was prepared via two steps, First step: copolymerization reaction of N-methacryloxyphtalimide (NMP) with methylenebisacrylamide (MBA) by suspension polymerization method to give ultrafine poly (NMP-co-MBA). Second step: reaction of triethylenetetramine (TETA) with poly (NMP-co-MBA) to give NSCR. The prepared NSCR was characterized by Fourier transform infrared spectroscopy (FT-IR), scanning electron microscopy (SEM), Transmission electron microscopy (TEM), Brunauer-Emmett-Taller (BET) and thermogravimetric analysis (TGA). This study illustrated the capability of NSCR for extraction of Cu(II), Co(II) and Ni(II) from aquatic solutions. The pH effect, metal ions concentration, temperature and contact time were elaborated in batch experiments. The results showed that high capacities were 1.3, 1.0 and 0.95 mmol/g resin for Cu(II), Ni(II) and Co(II) ions, respectively. The experimental data of adsorption isotherms were convenient for Langmuir isotherm, and the kinetic data illustrated that the removal process was described by pseudo-second order kinetic model. The parameters of Thermo dynamic illustrated that the process of adsorption was endothermic and spontaneous reaction. The prepared NSCR was regenerated and used repetitively for five times with small decrease in adsorption capacity.

Keywords Nanometer-sized chelating resin · N-methacryloxyphtalimide · Methylenebisacrylamide · SEM · TEM · Thermogravimetric analysis · Cu(II) · Ni(II) · Co(II) · Kinetics · Isotherms · Thermodynamics

✉ A. F. Shaaban
afshaaban@hotmail.com

A. A. Khalil
aamkhalil55@yahoo.com

Mohamed Radwan
Mohamed.aboelela2312@gmail.com

Manal El Hefnawy
manalelhefnawy@yahoo.com

H. A. El Khawaga
Hanaa.elkhawaga@gmail.com

[1] Chemistry Department, Faculty of Science, Benha University, Benha, Egypt

[2] Faculty of Engineering (Shoubra), Benha University, Shoubra, Egypt

Introduction

The pollution of water resources by industrial effluents which contain poisonous metal ions is a serious issue. High concentration of copper in water may district creatures like fish and molluscs [1]. Also, the exposure to copper for long time can effect on our health causing irritation to your nose and throat. When cobalt ions come in the atmosphere, they stabilize to the earth and enter the food and water and cannot be destroyed. When the body exposed to this metal, caused in oxidative stress, DNA damage and serious degenerative sickness. Now, patients with hip implants including cobalt are suffering from tinnitus, deafness, vertigo and blindness [2].

Nickel is considered one of heavy metals that pollute environment. Nickel exposure introduces free radicals which cause oxidative damage and may also affect the kidneys and liver [3]. The effective treatments of these toxic metal ions from the solution has received much attention owing to their toxicities low concentration and tendency to bioaccumulation [4, 5]. Nowadays, many processes were attainable for heavy metal extraction like liquid–liquid extraction, precipitation, electrolytic concentration, membrane filtration, ion exchange and adsorption [6–8], the last is generally preferred because of its high

qualification, ease of handling and availability of different organic sorbents involving chelating function groups [9–16].

In our previous work different chelating resins bearing amidoxime, imminodiacetate and dithiocarbamate groups were prepared for metal ions extraction from aquatic solution with high performance [17–20]. Nanoparticles are now being used as favorite adsorbent owing to their great surface area which is a very significant characteristic for a desired adsorbent. In the past decade, the improvement of nanoparticles has been the subject of interest. Ge et al. prepared novel Fe_3O_4 magnetic nanoparticles (MNPs) adjusted with 3-aminopropyltriethoxysilane (APS) and copolymers of acrylic acid (AA) and crotonic acid (CA) and exposed the cabapility of the MNPs for extracting of toxic metal ions Cd^{2+}, Zn^{2+}, Pb^{2+} and Cu^{2+} from aquuatic solution [21].

Nanoparticles of Polymer-supported hydrated iron(III) oxide were used for the extraction of both arsenates and arsenites [22]. A novel magnetic nano-adsorbent has been synthesized by the covalent immobilization of thiosalicylhydrazide on Fe_3O_4 nanoparticles. The ability of the synthesized MNPs for extracting heavy metals ions (Pb^{2+}, Cd^{2+}, Cu^{2+}, Zn^{2+}, and Co^{2+}) from industrial wastes was studied with large sorption capacities [23]. Wang et al. reported that all previous nano-sized adsorbent for metal ions extraction based on three kinds of nanomaterial's including nanocarbon materials, nanometal particles, and polymer-supported nanoparticles for metal ions extraction [24].

In the present work, it is worth mentioning here for the first time nanometer-sized chelating resin (NSCR) was prepared and characterized by different spectral techniques. The features of the NSCR surface were inspected by scanning electron microscopy (SEM). The sorption capacity of the synthesized NSCR towards Cu(II), Co(II) and Ni(II) ions was studied by batch technique. The factors affecting on the extraction of Cu(II), Co(II) and Ni(II) from aquatic solutions were studied as a function in pH of the solution, concentration of metal ions, contact time and temperature.

Experimental and characterization techniques

Materials

N-hydroxylphthalimide (NHP), methacrylic acid (MA) and N,N′-dicyclohexylcarbodiimide (DDC) were obtained from Merk Co., Germany. Methylenebisacrylamide (MBA), benzoyl peroxide, triethylenetetramine (TETA) and polyvinyl alcohol (PVA) were purchased from Sigma-Aldrish Co., USA. All solvents used were of reagent grade and were purified prior use. All other chemicals were used as received.

Method

Preparation of N-methacryloxyphthalimide (NMP)

NMP was prepared according to our previous work [25, 26]. In brief, NHP (32.6 g, 0.2 mol) and MA (41.2 g, 0.2 mol) were dissolved in well stirred cooled dry methylene chloride (300 ml), then N,N′-dicyclohexylcarbodiimide (DDC) (17.2 g, 0.2 mol) was dissolved in 100 ml of dry methylene chloride in a separate flask and was added drop wise to the reaction mixture. The reaction mixture was stirred for 6 h. The precipitated dicyclohexyl urea was then removed by filtration and the filtrate vaporized to dryness under vacuum using rotary evaporator. The residue obtained was recrystallized from benzene/petroleum ether (40–60 °C) mixture (20:80).

Synthesis of poly (NMP-co-MBA)

Poly (NMP-co-MBA) was prepared using suspension polymerization method. Copolymerization was conducted in a 250 mL round bottom, three-neck flask, fitted with a mechanical stirrer, nitrogen inlet and condenser. A mixture of 100 mL of 10% aqueous NaCl solution containing 0.1 g PVA was first introduced into the reactor, heated to the reaction temperature 90 °C, and stirred at 300 rpm for 1 h. A mixture of the monomer ratios NMP:MBA (4.5–3.0 g of NMP: 0.5–2.0 g of MBA) was dissolved in 15 ml ethyl acetate as a diluent, containing dibenzoyl peroxide as initiator (0.05 g; 1.0 wt% in relation to the monomers), was then added to the reactor under nitrogen atmosphere and the reaction was allowed to proceed for 24 h at 90 °C. After complete copolymerization, the ultrafine precipitate was collected using centrifuge and washed several times with distilled water, ethanol and acetone to remove PVA, NaCl, ethyl acetate and unreacted monomers and dried under vacuum at 60 °C. The conversion of poly (NMP-co-MBA) after purification is 96% (i.e. Almost all quantity of NMP (3 g, 0.013 mol) and MBA (2 g, 0.013 mol) monomers in the feed composition was copolymerized). Accordingly, the quantity of NMP and MBA are the same and ≈2.6 mmol/g of resin.

Synthesis of nanometer-sized chelating resin (NSCR)

NSCR were prepared by adding 5.03 ml of TETA to a mixture of 0.5 g of poly (NMP-co-MBA) and 10 ml toluene in a flask provided with a mechanical stirrer and reflux condenser. The reaction was stirred at 1200 rpm for 48 h at 100 °C. The obtained ultrafine precipitate of NSCR was collected using centrifuge and washed several times with ethanol and acetone to remove liberated NHP, residue of TETA and toluene and dried under vacuum at 60 °C to give 0.5649 g of NSCR after purification (i.e. Almost all quantity of poly (NMP-co-MBA) (0.5 g) was converted to NSCR). It means that the quantity of N,N-triethylenetetramine-bis-methacylamide repeating units in

Scheme 1 Schematic illustration of preparation process of NSCR

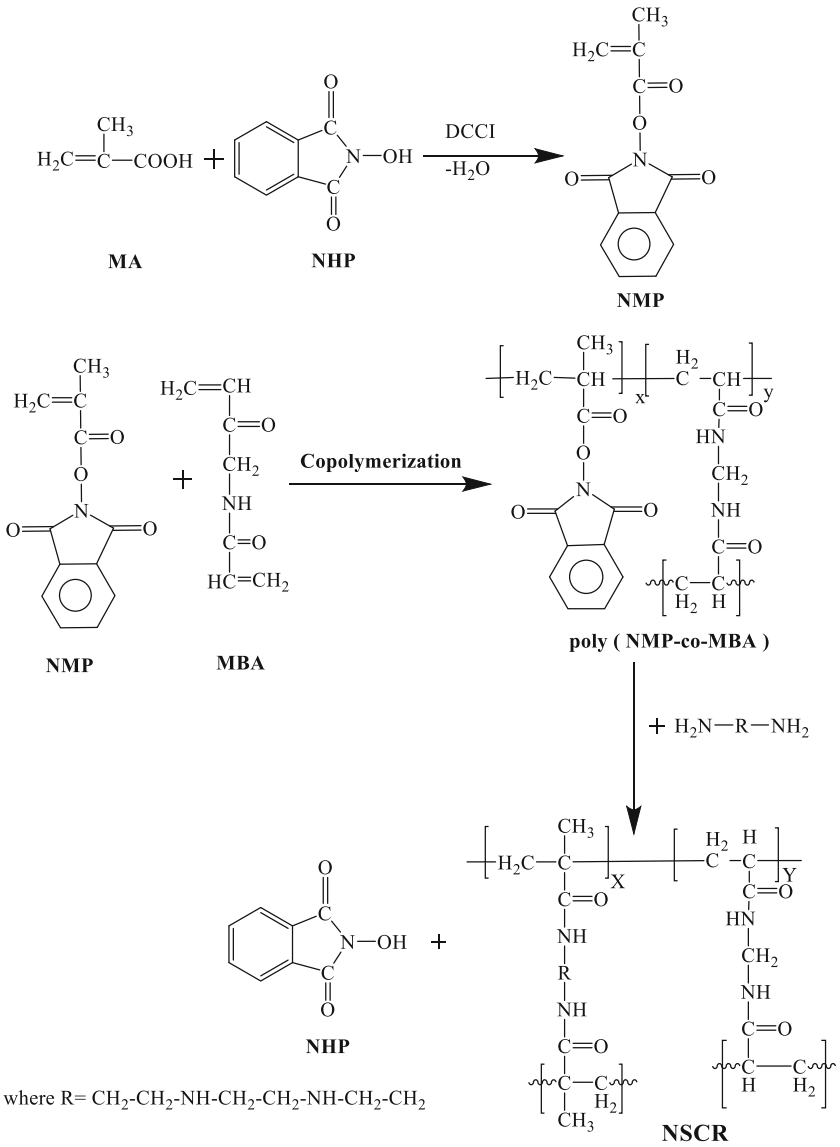

poly(N,N-triethylenetetramine-bis-methacylamide-co-MPA) [NSCR] is ≈2.3 mmol/g of resin.

Characterization techniques

FT-IR analysis

The synthesized NMP, poly (NMP-co-MBA) and NSCR were identified by FTIR using Shimadzu 8201 PC in the range of 400–4000 cm^{-1} in KBr phase.

Thermal analysis

TGA of the synthesized NSCR was determined using SDT Q600 V20.9 Build 20, USA. This experiment was performed from room temperature to 1000 °C in a dynamic atmosphere of nitrogen at nitrogen flow rate of 20 ml/min.

Surface area

Porous structure parameters of NSCR were described by Brunauer–Emmett–Teller (BET) and BJH methods through N_2 adsorption–desorption methods to inspect the porous properties of the NSCR using nitrogen as the adsorbent at 77.35 K. The measurements were excuted using a model NOVA 3200 automated gas sorption system (Quantachrome, USA).

Surface morphology of NSCR

Surface morphology of the synthesized NSCR and its metal complexes were determined by using QUANTA FEG scanning electron microscopy (SEM) at 40000 magnification and at 20 KV accelerating voltage.

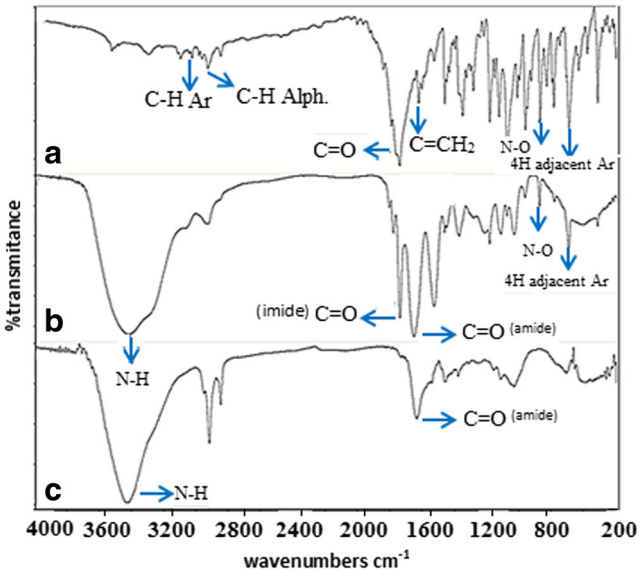

Fig. 1 FT-IR spectra of (**a**) NMP, (**b**) poly (NMP-co-MBA) and (**c**) NSCR

Transmission electron microscopy (TEM)

Morphology and particle size of NSCR was determined using transmission electron microscopy (TEM) (JEOL [JEM-1230 electron microscopy]). The sample was obtained as follows: ultrafine powder of sample was dispersed in water under ultrasonication, and then one drop of the suspension was suspended and evaporated on a carbon coated copper grid and placed in the Phillips (CM/TEM).

Adsorption of metal ions

Uptake of metal ions using batch method

All experiments were carried out using 0.1 g of NSCR in 250 ml conical flask containing 100 ml of single-metal ion solution and these experiments performed in a controlled shaker at 250 rpm. Also, all experiments were executed at 25 °C except the experiments of temperature. The pH was adjusted by adding few drops of HCl and/or NaOH solutions. Separation of NSCR from metal ions solution after adsorption experiments was carried out using centrifuge and the metal ion concentration in the supernatant solution was determined by Hitachi atomic absorption Z-6100 polarized Zeeman. Experiments were carried out in triplicate. The capacity of adsorption (q_e) in the equilibrium (mmol/g) was calculated by the next equation:

$$q = \frac{(C_o - C_e)V}{W} \quad (1)$$

where C_o and C_e are the initial and final concentration of metal ion solutions (mmol/l), V is the volume of metal ions solution (L), and W is the weight of dry resin (g).

Table 1 Porous structure parameters of NSCR

Parameters	NSCR
BET surface area (m^2/g)	365
BJH desorption average pore diameter (nm)	2.981
BJH desorption cumulative volume of pores (cm^3/g)	0.1500

Results and discussion

Synthesis of NSCR

NSCR were prepared via three steps presented in Scheme 1. In first step NMP monomer was prepared by the reaction of NHP with MA in the existence of DCC as dehydrating agent according to our previous work [25, 26]. The poly (NMP-co-MBA) was synthesized via copolymerization reaction of NMP

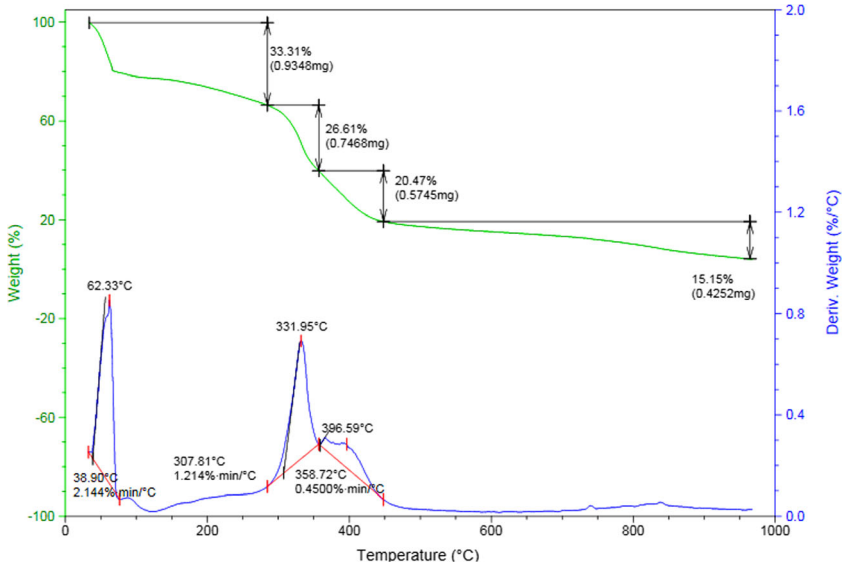

Fig. 2 TGA and DTA of the prepared NSCR

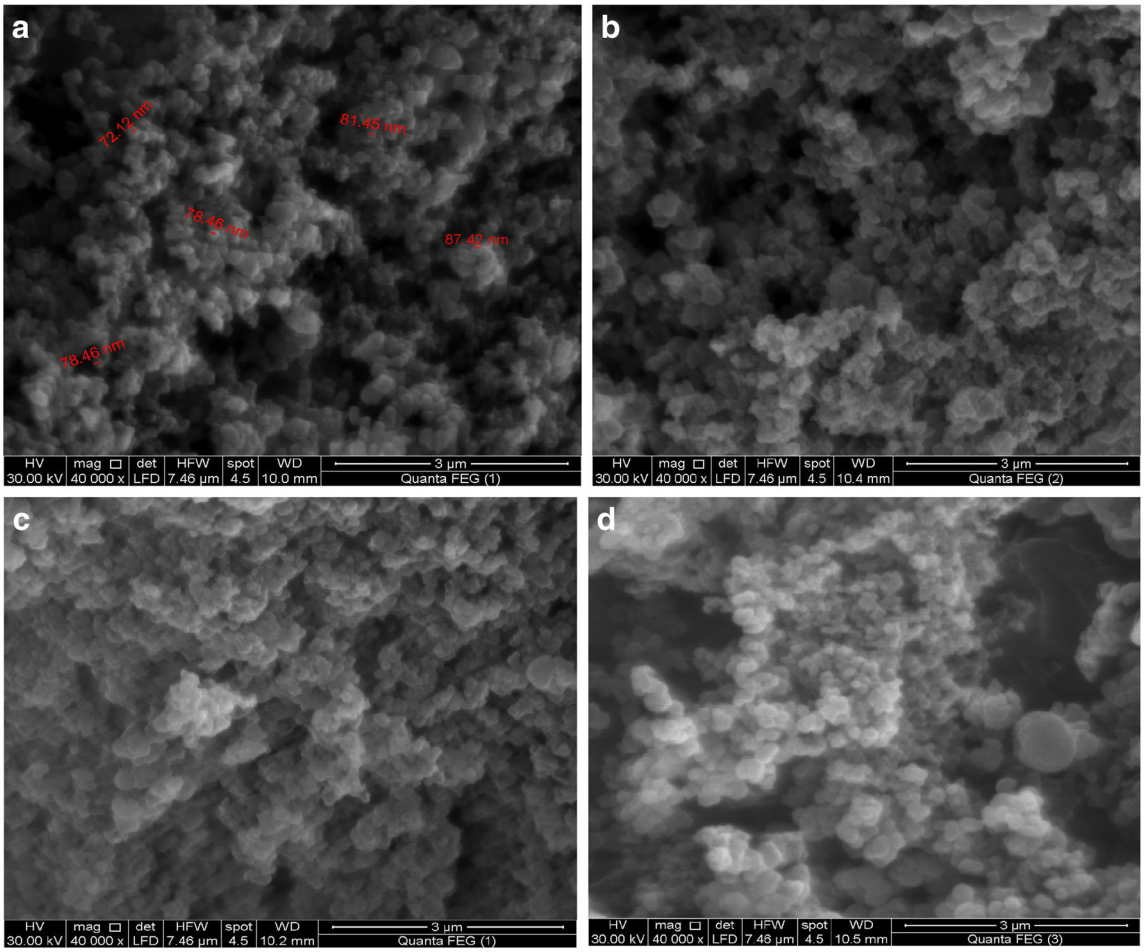

Fig. 3 SEM images of (**a**) NSCR, (**b**) NSCR-Cu, (**c**) NSCR-Co and (**d**) NSCR-Ni with magnification 40,000×

monomer with MBA as a cross-linking agent using suspension polymerization method. Finally NSCR was obtained by reaction of ultrafine precipitate of poly (NMP-co-MBA) with triethelenetetramine (TETA). Particle size of the prepared chelating resins depends on the quantity of cross-linked agent (MBA) in oil phase. In the range of MBA from 10 to 30% in relation to the monomer mixtures, the micrometer-sized chelating resins were obtained. On contrary in case of 40% MBA nanometer-sized chelating resin was obtained with diameter ranging from 72 to 87 nm.

Characterization of the synthesized resin

FT-IR of the prepared resin

FT-IR spectra of the prepared monomer and their resins were illustrated in Fig. 1a–c. IR spectrum of NMP monomer (Fig. 1a) showed band at 3102 cm^{-1} corresponding to C-H aromatic, a strong band at 2925 cm^{-1} of C-H aliphatic, a strong band at 1746 cm^{-1} related to C = O stretching frequency of phthalimide and C = O stretching of carboxylate carbonyl group. Also the IR spectrum showed band at 1627 cm^{-1} corresponding to the stretching frequency of the vinyldene group (C = CH_2), a strong band at 696 cm^{-1} corresponding to the four adjacent hydrogen atoms of the benzene ring and band at 930 cm^{-1} characteristic for N-O. IR spectrum of poly(NMP-co-MBA) (Fig. 1b) showed band at 3423 cm^{-1} due to N-H of amide group, two strong bands at 1742 and 1655 cm^{-1} characteristic for C = O of imide and amide groups, respectively, band at 696 cm^{-1} characteristic for the four adjacent hydrogen atoms of the benzene ring and band at 930 cm^{-1} characteristic for N-O. IR spectrum of NSCR (Fig. 1c) showed two bands at 3424 and 1638 cm^{-1} for N-H and C = O of amide group, respectively and disappearance the bands of aromatic (the four adjacent hydrogen atoms of the benzene ring at 696 cm^{-1}) and N-O group (930 cm^{-1}). It means that all phthaloxime moieties in NMP repeating units were disappeared (i.e. conversion/or exchange % is 100% for replacing phthaloxime groups by TETA moieties).

Thermal analysis

TGA was used to define the thermal stability of the NSCR. The TGA and DTA curves (Fig. 2) illustrated that the resin was degraded in four stages. The first stage from 32 to 282 °C

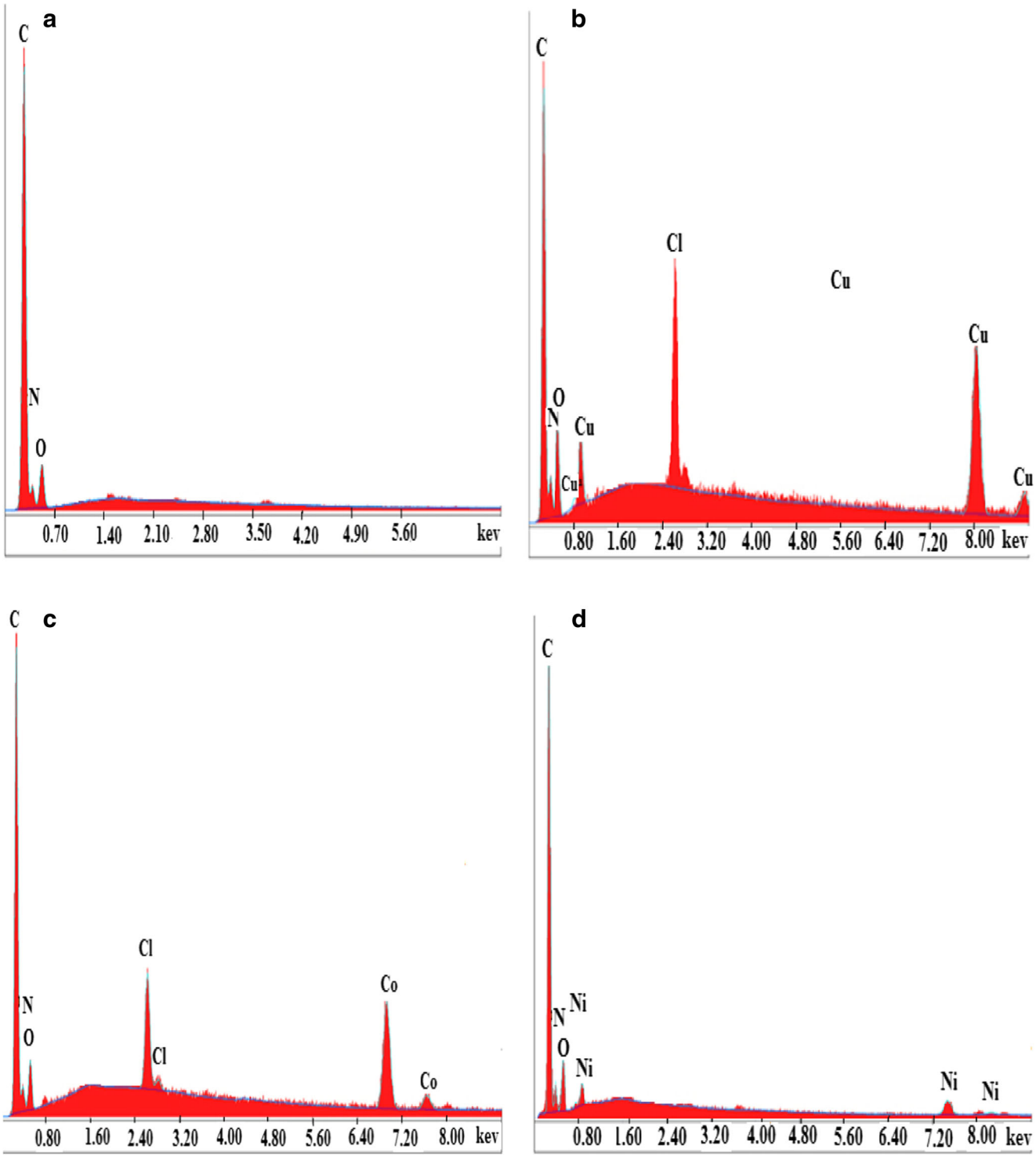

Fig. 4 EDX images of (**a**) NSCR, (**b**) NSCR-Cu, (**c**) NSCR-Co and (**d**) NSCR-Ni

with partial weight loss of 33.3% attributable to loss of water vapor and volatile materials which is present in external surface and internal pores or cavities of the resin. NSCR represents a novel class of hydrophilic hyper cross-linked polymers with mesoporous structure (2.981 nm) and higher surface area (365 m^2/g) that favor the adsorption of water vapor, volatile organic compounds (VOCs) [27] and polar compounds from water samples [28]. Therefore the sorption behavior of NSCR towards water vapor, VOCs and polar compounds such as residual acetone and ethanol that used in purification step of NSCR may be explained why the 20% weight loss of NSCR below 100 °C is notes in TGA curve. The second stage from

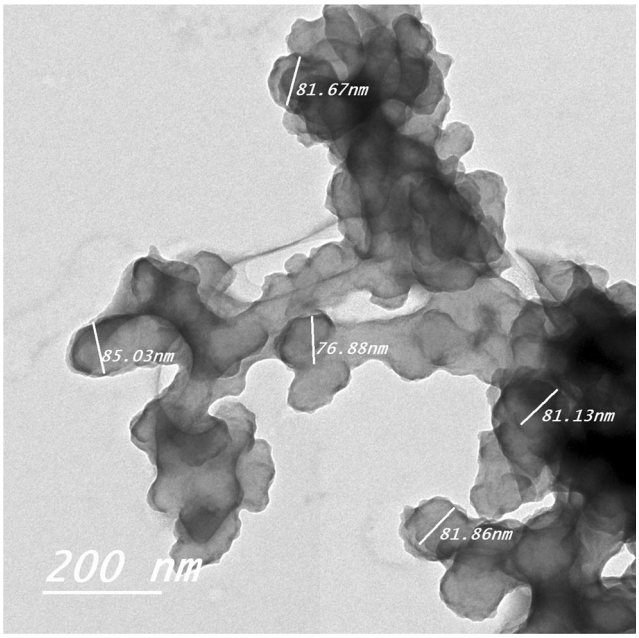

Fig. 5 TEM image of NSCR

282 to 356 °C with partial weight loss of 26.6% which assigned to degradation of grafted functional groups. The third stage from 356 to 445 °C with partial weight loss of 20.4%. The fourth stage from 445 to 960 °C with partial weight loss of 15.1%.Two latter weight losses can be attributed to decomposition of modifying, crosslinking agents and polymer chain.

Surface area

The BET surface area, BJH pore volume and average pore diameter for NSCR were determined (Table 1) by Brunauer–Emmett–Teller (BET) and BJH methods through N_2 adsorption–desorption methods at 77.35 K. These data illustrated that the NSCR had pore diameter 2.981 nm and pore volume 0.15 (cm^3/g) which to be considered mesoporous

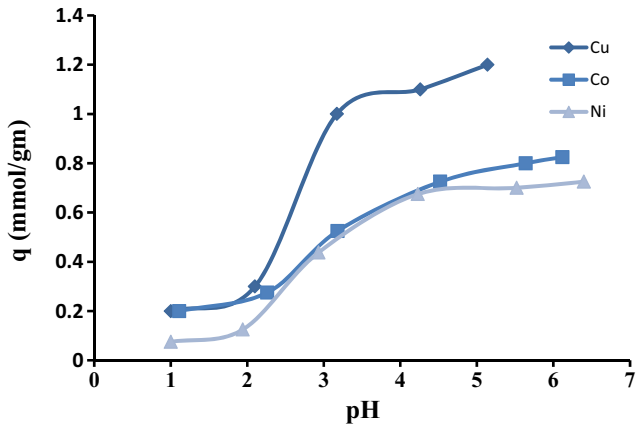

Fig. 6 Effect of pH on the uptake of metal ions; 25 °C, shaking time 3 h and initial metal ion concentration 5.0 mmol/l

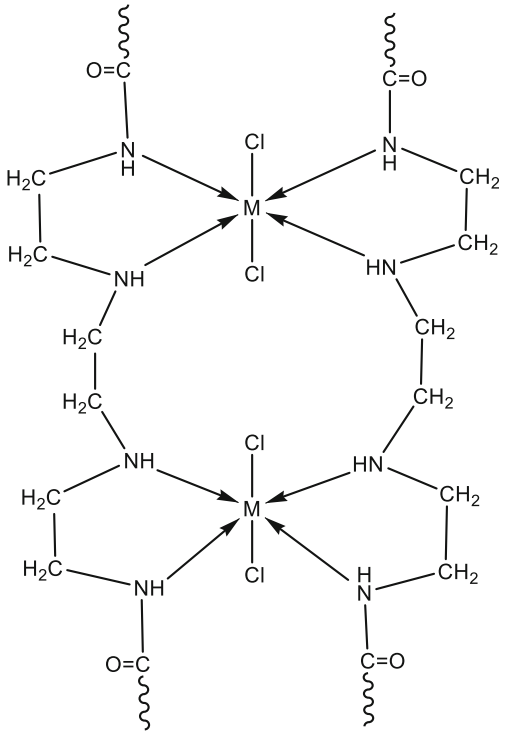

Scheme 2 Schematic illustration of chelation process of NSCR with metal ions based on TETA moieties

structure [29] and lead to efficient transfer the metal ions to the internal adsorption sites.

Scanning electron microscopy-EDX

The SEM images at 40000 magnifications for prepared NSCR and its metal complexes were presented in Fig. 3a–d. Fig. 3a showed the morphology of the resin before the adsorption of metal ions, which showed the particle size of the synthesized

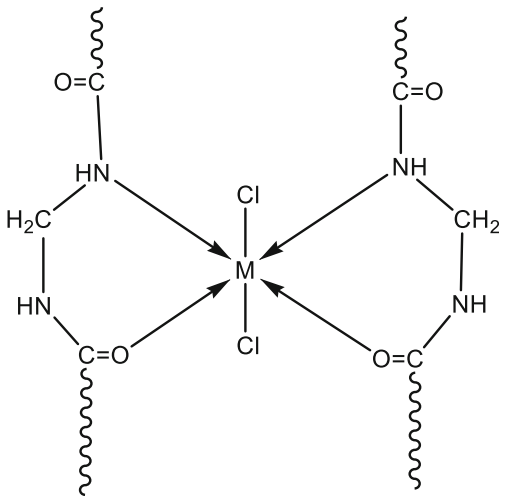

Scheme 3 Schematic illustration of chelation process of NSCR with metal ions based on MBA moieties

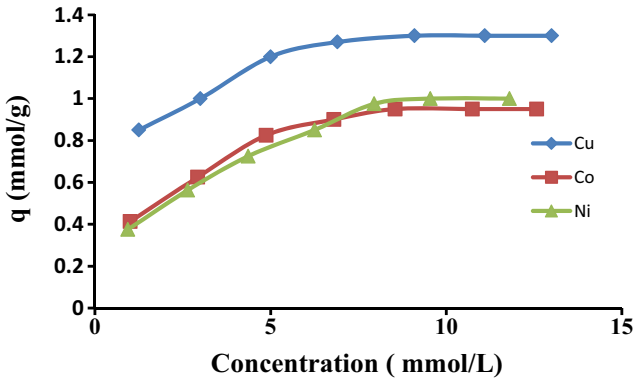

Fig. 7 Effect of initial metal ions concentration on the adsorption capacity of Cu(II), Co(II) and Ni(II); 25 °C, shaking time 3 h and at optimum pH value

resin in nano-scale with diameter ranging from 72 to 87 nm. After the adsorption of metal ions the particle size of the synthesized resin still in nano-scale as illustrated in Fig. 3b,c and d. The particles of NSCR before and after adsorption seem not isolated particles due to their agglomeration. However, very high surface area of these nanoscale particles offers favorable sorption process [30].

Fig. 4 showed EDX spectra for NSCR and its metal complexes. The presence of copper, cobalt and nickel with synthesized NSCR was confirmed from Energy dispersive X-ray spectroscopy (EDX) measurements. The NSCR with Cu(II), Co(II) and Ni(II) ions shows distinct signals at 0.9&8.0&8.9, 7.0&7.6 and 0.9&7.5&7.5 keV corresponding to Cu(II), Co(II) and Ni(II), respectively. The objective of this analysis was to map elemental Cu(II), Co(II) and Ni(II) qualitatively (not quantitatively) on the composite surface. However, the level of the Cu, Co and Ni signal observed was sufficient for providing a qualitative idea of the homogeneous distribution of Cu, Co and Ni element at the surface of the sorbent: the percentage (in mass) of Cu, Co and Ni was 17.3%, 9.74% and 2.61%, respectively.

Table 2 Comparison of maximum adsorption capacity of NSCR with those of some other chelating resins reported in literature for the adsorption of Cu(II), Co(II) and Ni(II)

Adsorbents	Metal ions	Sorption capacity (mmol/g)	Conditions	Ref.
Magnetic beads with amino groups	Cu(II) and Ni(II)	0.814 and 0.845	pH = 3–5 25 °C	[32]
Amidoximated grafted cellulose	Cu(II) and Ni(II)	1.6 and 0.84	pH = 5.5 30 °C	[33]
Amidoximated (AN/MA)	Cu(II) and Ni(II)	2.1 and 0.06	pH = 3 25 °C	[34]
PMHS-g-PyPzAllyl polymer & PMHS-g-PyPz(OEt)$_2$Allyl polymer	Cu(II),Ni (II) and Co(II)	1.48, 0.79 and 0.24 & 1.06, 0.58 and 0.57	pH = 5 25 ± 1 °C	[35]
Polyamine chelating resin (NDC-984)	Ni(II) and Co(II)	0.982 and 0.741	pH = 5 30 °C	[36]
Grafted poly(ethylene terephthalate) fiber	Cu(II),Ni (II) and Co(II)	0.49, 0.74 and 0.46	pH = 5 25 °C	[37]
Chitosan-grafted-poly(2-amino-4,5- pentamethylene-thiophene-3-carboxylic acid N -acryloyl-hydrazide)) (chitosan-g-ATAH) chelating resin	Cu(II),Ni (II) and Co(II)	2.36, 0.9 and 2.15	pH = 6 30 °C	[38]
Cross-linked magnetic chitosan–diacetylmonoxime Schiff's base resin (CSMO)	Cu(II), Co(II) and Ni(II)	1.5, 1.02 and 0.8	pH = 5 28 °C	[39]
2-minomethylpyridine molecule onto grafted silica gel (SiAMP)	Cu(II), Co(II) and Ni(II)	0.84, 0.67 and 0.40	25 ± 1 °C	[40]
Cross-linked magnetic chitosan-isatin Schiff's base resin (CSIS)	Cu(II), Co(II) and Ni(II)	1.62, 0.91, and 0.68	pH = 5 28 °C	[41]
NSCR	Cu(II), Co (II) and Ni(II)	1.3, 0.95 and 1	pH = 5.1, 6.1 and 6.4 25 °C	This work

Table 3 Parameters of Langmuir, Freundlich and Temkin isotherms for adsorption of metal ions on NSCR

Metal ion	Langmuir isotherm			Freundlich isotherm			Temkin isotherm		
	Q_{max}	K23	R^2	N	K_f	R^2	K_T	B	R^2
Cu(II)	1.360	2.277	0.9987	0.138	0.9598	0.9515	697.280	0.148	0.9460
Co(II)	1.058	0.876	0.9961	0.298	0.4998	0.9611	13.623	0.197	0.9646
Ni(II)	1.182	0.542	0.9863	0.456	0.3580	0.9852	7.307	0.233	0.9609

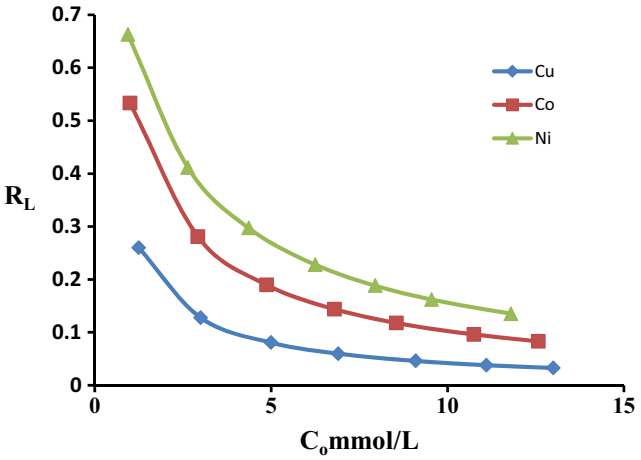

Fig. 8 Variation of adsorption intensity (R_L) with initial concentration (C_o)

Transmission electron microscopy

The TEM image at 200 nm for the prepared NSCR was presented in Fig. 5, which showed the particle size of the prepared resin in nano-scale with average diameter 81.3 nm.

Uptake of metal ions using batch method

Optimum pH of metal ions uptake

The optimum pH for sorption of Cu(II), Co(II) and Ni(II) ions was determined by shaking 0.1 g of resin with 100 ml of metal ion solution (5 mmol/l) for 3 h at 25 °C in pH ranging from 1 to 6.4. The results of this study were illustrated in Fig. 6. From these results, it was cleared that the sorption capacity of metal ions increased as pH increased, this is owing to the surface charge of nano particle becomes more negative at larger pH and hence the electrostatic attraction was increased between the resin and metal ion. The optimum pH for Cu(II), Co(II) and Ni(II) was 5.1, 6.1 and 6.4, respectively. After the optimum pH there is no high adsorption efficiency owing to the precipitation for all metal ions as metal(II) hydroxide.

$$M^{2+} + 2OH^- \rightarrow M(OH)_2\downarrow$$

The possible chelation models of NSCR with metal ions based on TETA and MBA moieties is presented in Schemes 2 and 3, respectively. It means that MBA repeating unit involved also in chelation with metal ions due to the presence of oxygen and nitrogen atoms in two amide groups of MBA repeating units. It means that MBA repeating units offer excellent opportunities conducive to increase adsorption of metal ions.

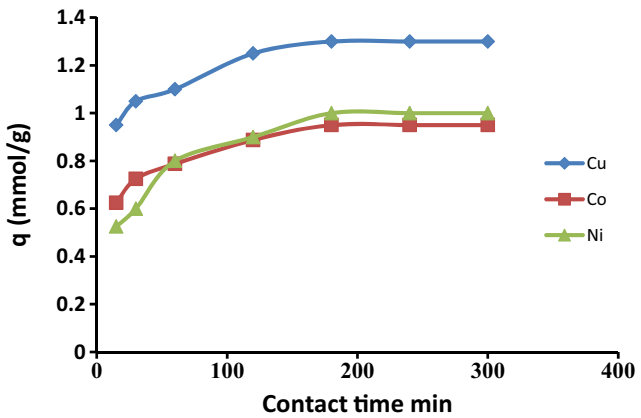

Fig. 9 Effect of shaking time on the adsorption capacity of Cu(II), Co(II) and Ni(II)

Effect of the initial concentration and equilibrium isotherm models

The effect of initial concentration of metal ions concentration was elaborated by shaking 0.1 g of NSCR with 100 ml of metal ion solution in a concentration ranging from 1 to 13 (mmol/l) at optimum pH and at 25 °C for 3 h, after that the resin was centrifuge and the concentration of the remaining metal ions solution was estimated from supernatant solution. The results were presented in Fig. 7. From these results, it was cleared that as the initial concentration of metal ions increased, the quantity of metal ion sorbed onto the resin increased. The optimum concentration of metal ions for Cu(II), Co(II) and Ni(II) were 9.1, 8.55 and 9.55 (mmol/l), respectively. Also, it was found that from Fig.7, the most adsorption of metal ion was in order of Cu(II) > Ni(II) ≥ Co(II). These differences in metal ions uptake are possibly related to the difference in ionic radius of these ions. The ionic radius of these metal ions is the order of Co(II) (0.74 Å) > Ni(II) (0.72 Å) > Cu(II) (0.69 Å) This means that the smaller the ionic radius, the higher the quantity of metal ions adsorbed [31]. Cu(II) was adsorbed more than Ni(II) and Co(II) by NSCR (Fig. 7) because of its smaller ionic radius since it is easily taking place in the pores of chelating resin (average pore diameter of NSCR equal to 2.981 nm). A comparison of the present NSCR with those of various types of adsorbents in other reported literatures is listed in Table 2.

The adsorption isotherm studies were used to determine the sorption capacity of metal ions. There are three commonly used isotherm models i.e. Langmuir, Freundlich, and Temkin isotherm. The Langmuir isotherm model equation is represented as [42]:

$$\frac{C_e}{q} = \frac{C_e}{Q_{max}} + \frac{1}{KQ_{max}} \quad (2)$$

where C_e is the equilibrium concentration of metal ions (mmol/l), q is the equilibrium adsorption capacity (mmol/g), Q_{max} (mmol/g) is the maximum adsorption capacity and K (l/mmol) is the Langmuir constant concerned to the affinity

Table 4 First-order, second-order and intra particle diffusion rate constants

Metal ion	Pseudo-first order kinetics			Pseudo-second-order kinetics			Intra particle diffusion	
	q (mmol/g)	K_{ads} (1/min)	R^2	Q	K_2	R^2	K_{id}	R^2
Cu(II)	0.476	0.01796	0.971	1.345	0.082	0.999	0.0265	0.8861
Co(II)	0.387	0.01500	0.992	0.991	0.088	0.999	0.0242	0.9089
Ni(II)	0.583	0.01500	0.977	1.076	0.047	0.999	0.0369	0.8979

of binding sites. The results of Langmuir equation were illustrated in Table 3.

The dimensionless constant separation factor (R_L) [43], which reflects the essential characteristic of the Langmuir model, can be determined according to the next equation:

$$R_L = \frac{1}{1 + KC_o} \quad (3)$$

where k is the Langmuir constant and C_o is the initial concentration of metal ion (mmol/l). The value of R_L which is calculated recommends the shape of the isotherm to be unfavorable ($R_L > 1$), linear (RL = 1), favorable ($0 < R_L < 1$), or irreversible ($R_L = 0$) [44, 45]. Plotting R_L versus Co is illustrated in Fig. 8. The calculated values of R_L were between zero and one for all metal ions detected that the adsorption of metal ions onto NSCR is favorable.

Another model which is used in this research is Freundlich model which described a heterogeneous adsorption system and illustrated by the next eq. [46]:

$$\log q = N \log C_e + \log K_F \quad (4)$$

where q is the equilibrium adsorption capacity (mmol/l), C_e is the equilibrium concentration of metal ions (mmol/l), K_F and N are Freundlich constants that give information about heterogeneity degree of the surface sites. These constants calculated from the slope and the intercept of the plot from log q_e versus log c_e and were collected in Table 2. The amount of N in Freundlich isotherm described the nature of isotherm, N >1 is unfavorable, 0< N > 1 is favorable or irreversible when $N = 0$. In this reserch the quantity of N for all metal ions between 0 and 1 referred that the metal ions adsorption on the resin was favorable.

The Temkin model isotherm is illustrated from the next eq. [47]:

$$q = B\,Ln\,k_T + B\,Ln\,C_e \quad (5)$$

where B is Temkin constant which represents the heat of adsorption and K_T is the equilibrium binding constant. The quantities of these constants were presented in Table 3. The parameters for Langmuir, Freundlich, Temkin isotherm and their correlation coefficients values were located in Table 3. As shown in Table 3, the experimental data were more favorable with Langmuir, Freundlich, and Temkin isotherm models and high correlation coefficient (R^2) obtained for these plots indicates the validity of these models to NSCR for these metals ions. But Langmuir model illustrates better results than Freundlich and Temkin models owing to larger correlation coefficient for these metal ions.

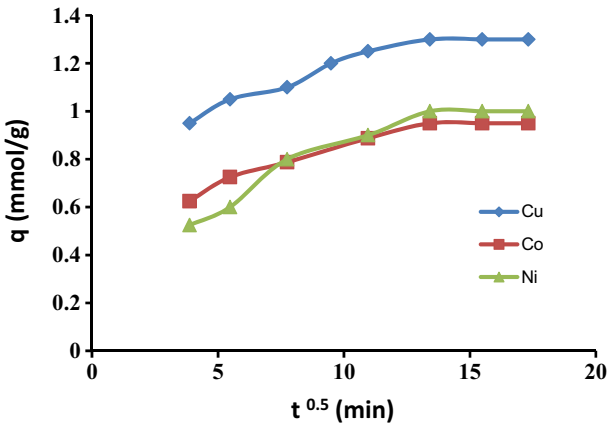

Fig. 10 Plot of Weber-Morris intra particle diffusion model for the adsorption of metal ions on nano-chelating resin

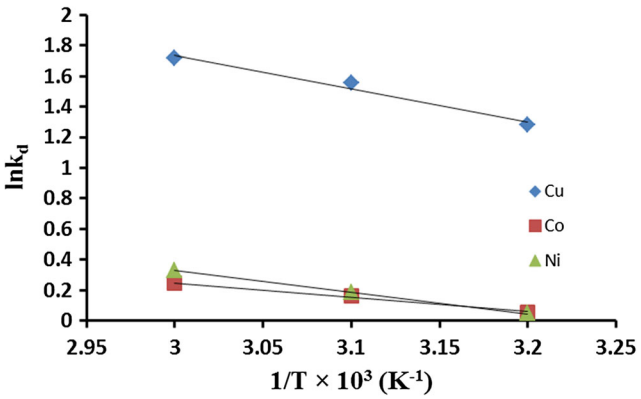

Fig. 11 Plot of $\ln k_d$ vs 1/T for adsorption of metal ions on NSCR

Table 5 Thermodynamic parameters for the adsorption of metal ions onto chelating resin

Metal ion	$-\Delta G^{o}_{ads}$ (KJ/mol)			ΔH^{o}_{ads} (KJ/mol)	ΔS^{o}_{ads} (J/mol)	R^2
	328 K	318 K	308 K			
Cu(II)	4.68	4.12	3.280	18.15	68.897	0.976
Co(II)	0.67	0.430	0.14	7.93	25.870	0.994
Ni(II)	0.896	0.49	0.12	11.73	37.910	1.000

Adsorption kinetics

To study the effect of contact time between NSCR and aqueous solution of metal ions adsorption, variations of adsorption capacity (q_e) vs time were shown in Fig. 9. It was found that, the adsorption of metal ions from aquatic solution using the adsorbent is continuously increased with time increase until attaining equilibrium between two phases after 3 h. Therefore, this optimum equilibrium time was selected for the next adsorption experiment. The adsorption results were used to inspect the kinetic mechanism which controls the adsorption process. The most widely used models of Lagergren's pseudo-first order; pseudo-second order and intra particle diffusion were used to examine the kinetic process [48–50]. The linear form of the first order rate equation by Lagergren and Svenska [48] is illustrated in Eq. (6):

$$\log(q-q_t) = \log q - \left(\frac{k_{ads}}{2.303}\right)t \tag{6}$$

The pseudo-second order kinetic model of Ho [49] can be presented as follow:

$$\frac{t}{q_t} = \frac{1}{k_2 q^2} + \left(\frac{1}{q}\right)t \tag{7}$$

where q and q_t, the quantity of metal ion adsorbed (mmol/g) at equilibrium and at time t (min), respectively, K_{ads} is lagergren rate constant (min^{-1}) of the adsorption and K_2 is the pseudo-second order rate constant. The intra particle diffusion is proposed by Weber and Morris [50] was obtained by the next equation:

$$q_t = K_{id} t^{0.5} \tag{8}$$

where k_{id} is the intra particle diffusion rate constant ($mmolg^{-1}/min^{0.5}$). The constants of first order, second order and intra particle diffusion model were listed in Table 4. The kinetic data described that the sorption process for all metal ions was described by pseudo-second order kinetic model. When the plot q_t against $t^{0.5}$ gives straight line, this means that the intra particle diffusion represented as the only rate limiting step, but when the plot gives multi-linearity indicates two or more stages for the metal ions adsorption [51]. In Fig. 10, the adsorption process involves three steps, (**a**) external film diffusion: diffusion of metals ion to the surface of nano-chelating resin, (**b**) intra particle diffusion: metal ions transfer from the external surface of the resin to the internal pores of the resin through intra particle diffusion; and (**c**) interaction between metal ions and the active sites of the resin which is the final equilibrium step.

Adsorption thermodynamics

The adsorption experiments were carried out at three different temperatures (35, 45 and 55 °C) to calculate parameters of thermo dynamic. In these experiments, metal ion solution (100 ml of 1 mmol/l) with 0.1 g of NSCR was used at optimum pH.

Equilibrium distribution coefficient for adsorption process, k_d, was calculated by the next eq. [52].

$$K_d = \frac{(C_o - C_e)}{C_e} \times \frac{V}{W} \tag{9}$$

where c_o and c_e are the initial and equilibrium concentration of metal ion (mmol/l), V is the total volume of solution in (L) and, W the weight of the NSCR in (g).

Free energy change of the adsorption (ΔG^{o}_{ads}) was studied using the next equation:

$$\Delta G^{o}_{ads} = -RT \ln k_d \tag{10}$$

The standard enthalpy change (ΔH^{o}_{ads}) and entropy change (ΔS^{o}_{ads}) of the adsorption were estimated by plotting $\ln K_d$ versus 1/T (Fig. 11) according to Eq. (11).

$$\ln k_d = \frac{\Delta S^{o}ads}{R} - \frac{\Delta H^{o}ads}{RT} \tag{11}$$

where R is gas constant (8.314 J/mol k). The amounts of ΔH^{o}_{ads} and ΔS^{o}_{ads} were obtained from the slope and the intercept, respectively.

The parameters of thermodynamic of ΔG^{o}_{ads}, ΔH^{o}_{ads} and ΔS^{o}_{ads} were displayed in Table 5. The positive quantities of ΔH^{o}_{ads} refer that metal ion adsorption were an endothermic process [53, 54]. The positive quantities of ΔS^{o}_{ads} may be concerned to the release of water of hydration through the process of adsorption which

causing an increase in the randomness of the system [53, 54]; while the negative values of ΔG^{o}_{ads} indicate that the sorption process was spontaneous. The increase in negative values of ΔG^{o}_{ads} with temperature refer to the adsorption was more favorable at high temperature.

The regeneration of loaded NSCR with Cu(II), Co(II) and Ni(II) was studied using 0.2 M HNO_3 at 25 °C. To check the reusability of NSCR, five successive adsorption- desorption cycles were performed. The results reffered that the adsorption capacity decreased from 100% to 98, 97, 96, 94 and 92% respectively over five cycles.

Conclusion

In this study, new nanometer-sized chelating resin was prepared and characterized. The morphology of the synthesized chelating resin was characterized using scanning electron microscopy (SEM) and transmission electron microscopy (TEM), which showed the particle size of resin in nano-size scale. This resin showed good adsorption capacity toward Cu(II), Co(II) and Ni(II) from their aqueous solutions. Batch experiments were carried out to study the influences of pH, initial concentration, adsorption time and temperature. The nano-chelating resin showed high adsorption capacity for metals corresponding to the next order Cu(II) > Ni(II) > Co(II). From the results, it was illustrated that Langmuir isotherm model is more favorable for adsorption isotherm of these metal ions. The kinetic data described well by the bseudo-second order model. The thermo dynamic parameters ΔG^{o}_{ads}, ΔH^{o}_{ads} and ΔS^{o}_{ads} were studied. The quantities of ΔG^{o} and ΔH^{o} indicate the process of adsorption is endothermic and spontaneous in nature. The resin was regained by using 0.2 M HNO_3 and the resin could be used for 5 times.

References

1. Van Genderen EJ, Ryan AC, Tomasso JR, Klaine SJ (2005) Evaluation of acute copper toxicity to larval fathead minnows (Pimephales Promelas) in soft surface waters. Environ Toxicol Chem 24:408–414
2. Apostoli P, Catalani S, Zaghini A, Mariotti A, Poliani PL, Vielmi V, Semeraro F, Duse S, Porzionato A, Macchi V, Padovani A, Rizzetti MC, De Caro R (2012) High doses of cobalt induce optic and auditory neuropathy. Exp Toxicol Pathol 65:719–727
3. Das KK, Das SN, Dhundasi SA (2008) Nickel, its adverse health effects & oxidative stress. Indian J Med Res 128:412–425
4. Nebel BJ, Wright RT (1966) Environmental science 5th edn. Prenticehall, London,
5. Nagh WSW, Endud CS, Mayanar R (2002) Removal of Cu(II) ions from aqueous solution onto chitosan and crosslinked chitosan beads. React Funct Polym 50:181–190
6. Tofighy MA, Mohammadi T (2011) Adsorption of divalent heavy metal ions from water using carbon nano tube sheet. J Hazard Mater 185:140–147
7. Deligz H, Erdem E (2008) Comparative studies on the solvent extraction of transition metal cations by calixarene, phenol and ester derivatives. J Hazard Mater 154:29–32
8. Bessbousse H, Rhlalou T, Verchere JF, Lebrun L (2008) Removal of heavy metal ions from aqueous solutions by filteration with a novel complexing membrane containing poly(ethyleneimine) inapoly (vinylalcohol) matrix. J Membr Sci 307:249–259
9. Rivas BL, Quilodran B, Quiroz E (2004) Trace metal ion retention properties of crosslinked poly(4-Vinylpyridine) and poly(acrylic acid). J Appl Polym Sci 92:2908–2916
10. Henry WD, Zhao D, Sengupta AK, Lang C (2004) Preparation and characterization of a new class of polymeric ligand exchangers for selective removal of trace contaminants from water. React Funct Polym 60:109–120
11. Nastasovic A, Jovanovic S, Dordevic D, Onjia A, Jakovljevic D, Novakovic T (2004) Metal sorption on macroporous poly (GMA-co-EGDMA) modified with ethylene di amine. React Funct Polym 58:139–147
12. Baraka A, Hall PJ, Heslop MJ (2007) Preparation and characterization of melamine-formaldehyde-dtpa chelating resin and its use as an adsorbent for heavy metals removal from wastewater. React Funct Polym 67:585–600
13. Leinonen H, Lehto J (2000) Ion-exchange of nickel by iminodiacetic acid chelating resin Chelex 100. React Funct Polym 43:1–6
14. Neagu V, Bunia I, Luca C (2006) Organic ion exchangers synthesis and their behaviour in the retention of some metal ions. Macromol Symp 235:136–142
15. Denizli A, Sanli N, Garipcan B, Patir S, Alsancak G (2004) Methacryloylamidoglutamic acid incorporated porous poly(methyl methacrylate) beads for heavy-metal removal. Ind Eng Chem Res 43:6095–6101
16. Zohuriaan Mehr MJ, Pourjavadi A, Salehi Rad M (2004) Modified CMC. 2. Novel carboxymethylcellulose-based poly(amidoxime) chelating resin with high metal sorption capacity. React Funct Polym 61:23–31
17. Shaaban AF, Fadel DA, Mahmoud AA, Elkomy MA, Elbahy SM (2014) Synthesis of a new chelating resin bearing amidoxime group for adsorption of cu(II), Ni(II) and Pb(II) by batch and fixed-bed column methods. J Environ Chem Eng 2:632–641
18. Shaaban AF, Fadel DA, Mahmoud AA, Elkomy MA, Elbahy SM (2013) Removal of Pb(II), cd(II), Mn(II) and Zn(II) using iminodiacetate chelating resin by batch and fixed bed column methods. Desalin Water Treat 51:5526–5536
19. Shaaban AF, Fadel DA, Mahmoud AA, Elkomy MA, Elbahy SM (2013) Synthesis and characterization of dithiocarbamate chelating resin and its adsorption performance towards Hg(II), Cd(II) and Pb(II) by batch and fixed-bed column methods. J Environ Chem Eng 1:208–217
20. Shaaban AF, Mohamed TY, Fadel DA, Bayomi NM (2017) Removal of Ba(II) and Sr(II) ions using modified chitosan beads with bendent amidoxime moieties by batch and fixed column methods. J Desalin Water Treat in press
21. Ge F, Li M, Ye H, Zhao B (2012) Effective removal of heavy metal ions Cd^{2+}, Zn^{2+}, Pb^{2+}, Cu^{2+} from aqueous solution by polymer-modified magnetic nanoparticles. J Hazard Mater 211–212:366–372
22. Cumbal L, Sengupta AK (2005) Removal using polymer-supported hydrated iron(III) oxide nanoparticles: role of donnan membrane effect. Environ Sci Technol 39:6508–6515

23. Zargoosh K, Abedini H, Abdolmaleki A, Molavian MR (2013) Effective removal of heavy metal ions from industrial wastes using thiosalicylhydrazide-modified magnetic nanoparticles. Ind Eng Chem Res 52:14944–14954
24. Wang X, Guo Y, Yang L, Han M, Zhao J, Cheng X (2012) Nanomaterials as sorbents to remove heavy metal ions in wastewater treatment. J Environ Anal Toxicol 2:154
25. Shaaban AF, Arief MMH, Khalil AA, Messina NN (1988) 2-Poly-N-acyloyloxy- and -N- methacryloyloxyphthalimi- de as activated drug-binding matrices. Acta Polym 39:145–148
26. Khalil AA (2006) Exchange reactions of poly-2-(N-phthalimido) ethyl acrylate with hydroxyl and amino compounds. J Appl Polym Sci 99:2258–2262
27. Long C, Li Y, Yu W, Li A (2012) Adsorption characteristics of water vapor on the hypercrosslinked polymeric adsorbent. Chem Eng J 180:106–112
28. Bratkowska D, Fontanals N, Borrull F, Cormack PAG, Sherrington DC, Marce RM (2010) Hydrophilic hypercrosslinked polymeric sorbents for the solid-phase extraction of polar contaminants from water. J Chromatogr A 1217:3238–3243
29. Gurses A, Yalcin M, Sozbilir M, Dogar C (2003) The investigation of adsorption thermodynamics and mechanism of a cationic surfactant, CTAB, onto powdered active carbon. Fuel Process Technol 81:57–66
30. Cumbal L, Greenleaf J, Leun D, SenGupta AK (2003) Polymer supported inorganic nanoparticles: characterization and environmental applications. React Funct Polym 54:167–180
31. Elbhiri Z, Chevalier Y, Chovelon J-M, Jeffrezic-Renault N (2000) Grafting of phosphonate groups on the silica surface for the elaboration of ion-sensitive field-effect transistors. Talanta 52:495–507
32. Lin Z, Zhang Y, Chen Y, Qian H (2012) Extraction and recycling utilization of metal ions ($Cu^{2+,}$ Co^{2+} and Ni^{2+}) with magnetic polymer beads. J Chem Eng 200–202:104–110
33. Pekel N, Sahiner N, Guven O (2001) Use of amidoximated acrylonitrile/N-vinyl 2 pyrrolidone interpenetrating polymer networks for uranyl ion adsorption from aqueous systems. J Appl Polym Sci 81:2324–2329
34. Kawai O, Saito K, Sugita K (2000) Comparison of amidoxime adsorbents prepared by cografting methacrylic acid and 2-hydroxyethyl methacrylate with acrylonitrile onto polyethylene. Ind Eng Chem Res 39:2910–2915
35. Cegłowski M, Schroeder G (2015) Removal of heavy metal ions with the use of chelating polymers obtained by grafting pyridine–pyrazole ligands onto polymethylhydrosiloxane. J Chem Eng 259:885–893
36. Lia B, Liu F, Wang J, Ling C, Li L, Hou P, Li A, Bai Z (2012) Efficient separation and high selectivity for nickel from cobalt-solution by a novel chelating resin: batch, column and competition investigation. J Chem Eng 195–196:31–39
37. Coşkun R, Soykan C, Saçak M (2006) Adsorption of copper(II), nickel(II) and cobalt(II) ions from aqueous solution by methacrylic acid/acrylamide monomer mixture grafted poly(ethylene terephthalate) fiber. Sep Purif Technol 49:107–114
38. Bekheit MM, Nawar N, Addison AW, Abdel-Latif DA, Monier M (2011) Preparation and characterization of chitosan-grafted-poly(2-amino-4,5-pentamethylene-thiophene-3-carboxylic acid N -acryloyl-hydrazide) chelating resin for removal of Cu(II), Co(II) and Ni(II) metal ions from aqueous solutions. Int J Biol Macromol 48:558–565
39. Monier M, Ayad DM, Wei Y, Sarhan AA (2010) Preparation and characterization of magnetic chelating resin based on chitosan for adsorption of Cu(II), Co(II), and Ni(II) ions. React Funct Polym 70:257–266
40. Sales Jose AA, Faria Flavia P, Prado Alexandre GS, Claudio A (2004) Attachment of 2-aminomethylpyridine molecule onto grafted silica gel surface and its ability in chelating cations. Polyhedron 23:719–725
41. Monier M, Ayad DM, Wei Y, Sarhan AA (2010) Adsorption of Cu(II), Co(II), and Ni(II) ions by modified magnetic chitosan chelating resin. J Hazard Mater 177:962–970
42. Langmuir I (1918) The adsorption of gases on plane surfaces of glass, mica and platinum. J Am Chem Soc 40:1361–1403
43. Weber TW, Chakravot RK (1974) Pore and solid diffusion models for fixed bed adsorbents. AICHE J 20:228–238
44. Sari A, Tuzen M, Citak D, Soylak M (2007) Equilibrium, kinetic and thermodynamic studies of adsorption of Pb(II) from aqueous solution onto Turkish kaolinite clay. J Hazard Mater 149:283–291
45. Wang XS, Huang J, Hua HQ, Wang J, Qin Y (2007) Determination of kinetic and equilibrium parameters of the batch adsorption of Ni(II) from aqueous solutions by Na-mordenite. J Hazard Mater 142:468–476
46. Freundlich H (1906) Adsorption in solution. Phys Chem Soc 40: 1361–1368
47. Temkin MJ, Phyzev V (1940) Recent modifications to Langmuir isotherms. Acta Physiochim 12:217–222
48. Lagergren S, Svenska BK (1898) Zur theorie der sogenannten adsorption geloester stoffe. K Svenska Vetenskapsakad Handl 24:1–39
49. Ho YS (2006) Second order kinetic model for the sorption of cadmium on to tree fern: a comparison of linear and non linear methods. Water Res 40:119–125
50. Weber WJ, Morris JC (1964) Equilibria and capacities for adsorption on carbon. J Sanit Eng Div 90:79–91
51. Sarici-Ozdemir C, Onal Y (2010) Equilibrium, kinetic and thermodynamic adsorptions of the environmental pollutant tannic acid onto activated carbon. Desalination 251:146–152
52. Nilchi A, Saberi R, Moradi M, Azizpour H, Zarghami R (2011) Adsorption of cesium on copper hexacyanoferrate–PAN composite ion exchanger from aqueous solution. J Chem Eng 172:572–580
53. Unlu N, Ersoz M (2007) Removal of heavy metal ions by using dithiocarbamated- sporopollenin. Sep Purif Technol 52:461–469
54. Bandegharaei AH, Hosseini MS, Jalalabadi Y, Sarwghadi M, Nedaie M, Taherian A, Ghaznavi A, Eftekhari A (2011) Removal of Hg (II) from aqueous solutions using a novel impregnated resin containing 1-(2-thiazolylazo)-2-naphthol (TAN). J Chem Eng 168:1163–1173